JACS
JOURNAL OF THE AMERICAN CHEMICAL SOCIETY
Article
pubs.acs.org/JACS

A Detailed Study of Acetate-Assisted C−H Activation at Palladium(IV) Centers

Ansis Maleckis, Jeff W. Kampf, and Melanie S. Sanford*

Department of Chemistry, University of Michigan, 930 North University Avenue, Ann Arbor Michigan 48109, United States

Supporting Information

ABSTRACT: This report describes a detailed investigation of acetate-assisted C−H activation at Pd^{IV} centers supported by the tris(2-pyridyl)-methane (Py_3CH) ligand. Mechanistic information about this transformation has been obtained through the following: (i) extensive one- and two-dimensional NMR analysis, (ii) reactivity studies of a series of substituted analogues, and (iii) isotope effect studies. These experiments all suggest that C−H activation at $[(Py_3CH)Pd^{IV}(biphenyl)Cl_2]^+$ occurs via a multistep process involving chloride-to-acetate ligand exchange followed by conformational and configurational isomerization and then C−H cleavage. The data also suggest that C−H cleavage proceeds via an acetate-assisted mechanism with the carboxylate likely serving as an intramolecular base. The viability of acetate-assisted C−H activation at high valent palladium has important implications for the design and optimization of catalytic processes involving this transformation as a key step.

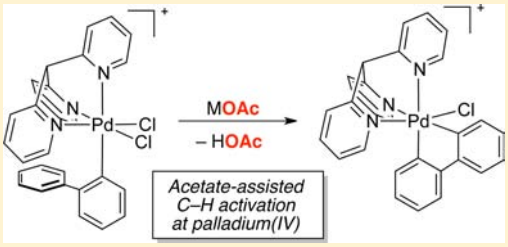

INTRODUCTION

Over the past decade, palladium-catalyzed C−H bond functionalization reactions have emerged as valuable methods in organic synthesis.[1] The vast majority of these transformations are believed to involve C−H activation at a Pd^{II} center.[1a] In these systems, $Pd(OAc)_2$ is typically used as the catalyst (often in conjunction with a carboxylate salt or carboxylic acid solvent), and the carboxylate plays an intimate role in the C−H cleavage process. Numerous studies have implicated cyclic transition states for C−H activation at Pd^{II}, where the carbonyl group of the carboxylate ligand acts as an internal base (eq 1, **1**).[2,3] This carboxylate-assisted

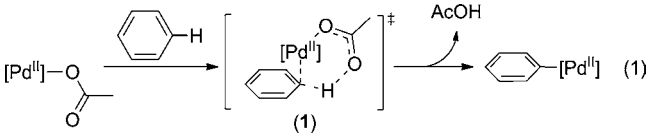

C−H cleavage pathway is supported by extensive experimental data as well as quantum-mechanical calculations.[4,5] DFT suggests that there is minimal charge buildup in transition state **1** and that the association between Pd^{II} and the C−H bond can be described as an agostic interaction rather than a π-delocalized Wheland-type species.[4,5] Recent work has shown that carboxylate-assisted C−H cleavage can also occur at Rh^{III}, Ir^{III} and Ru^{II} centers.[1b,6−8]

While carboxylate-assisted C−H activation at Pd^{II} has been well studied, the possibility of analogous pathways at high oxidation state palladium (Pd^{III} and/or Pd^{IV}) centers remains unexplored. This gap is particularly noteworthy because C−H activation at transient Pd^{IV} intermediates has recently been proposed as a key step in a number of different catalytic transformations.[9] In most of these cases, palladium carboxylates were used as catalysts, suggesting the possibility for acetate-assisted pathways. However, these transformations often proceed with markedly different site selectivity than Pd^{II}-mediated C−H functionalization processes.[9] Thus, it is of great importance to understand whether these differences are the result of novel mechanistic pathways for C−H activation at Pd^{IV}, different ligand environments at octahedral Pd^{IV} versus square planar Pd^{II} complexes, or other factor(s).

This paper describes the design of Pd^{IV} model complexes that have enabled a detailed interrogation of C−H activation at a Pd^{IV} center. We demonstrate the first characterized example of carboxylate-assisted C−H cleavage at Pd^{IV} and propose a mechanism for this transformation that is supported by a series of experiments. The studies and mechanistic insights obtained herein could ultimately prove valuable in accelerating the design and optimization of catalytic processes involving C−H activation at high valent Pd as a key step.

RESULTS AND DISCUSSION

A recent communication from our group described the first example of C−H activation at a Pd^{IV} center.[10] In that system, the oxidation of Pd^{II} precursor **2** with $PhICl_2$ at −35 °C afforded Pd^{IV} complex **3** as a transient intermediate. Warming a solution of **3** to 25 °C resulted in rapid C−H activation to generate cyclopalladated product **4** (eq 2). Coordinatively unsaturated cationic

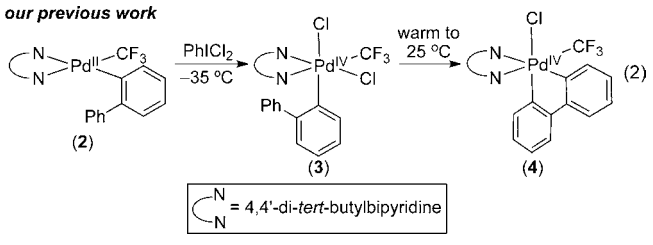

Received: February 12, 2013
Published: April 19, 2013

dx.doi.org/10.1021/ja401557m | J. Am. Chem. Soc. 2013, 135, 6618−6625

Pd^{IV} species like **5** or **6** (Figure 1) are likely intermediates in the conversion of **3** to **4**; however, the low stability of **3** hampered more detailed mechanistic investigations of this transformation.

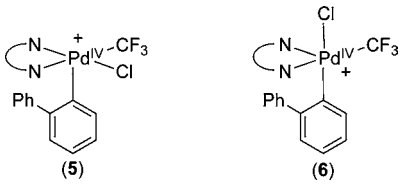

Figure 1. Putative cationic Pd^{IV} intermediates.

Design of Complexes for Mechanistic Study. We hypothesized that replacing the bidentate 4,4′-di-*tert*-butylbipyridine ligand with a tridentate supporting ligand would stabilize analogues of **5** and **6**, thereby enabling a thorough mechanistic investigation of the C−H activation reaction. Use of multidentate ligands is a common strategy to stabilize high-valent Pd complexes.[11−13] For example, Canty and co-workers have previously reported several organometallic Pd^{IV} tris(2-pyridyl)methane (Py_3CH) complexes that are stable to reductive elimination at room temperature.[14] This suggested that the third pyridine arm of Py_3CH might impart an appropriate balance of stability and reactivity to enable C−H activation at Pd^{IV}. The Py_3CH ligand was prepared in one step from α-picoline and 2-fluoropyridine (see Supporting Information for complete details).

Synthesis of Pd^{II}-σ-Aryl Complexes. Our initial synthetic efforts targeted Pd^{IV} complexes of general structure $[(Py_3CH)Pd(biphenyl)Cl_2]^+$ (eq 3). The treatment of $(Py_3CH)Pd^{II}$(biphenyl)-

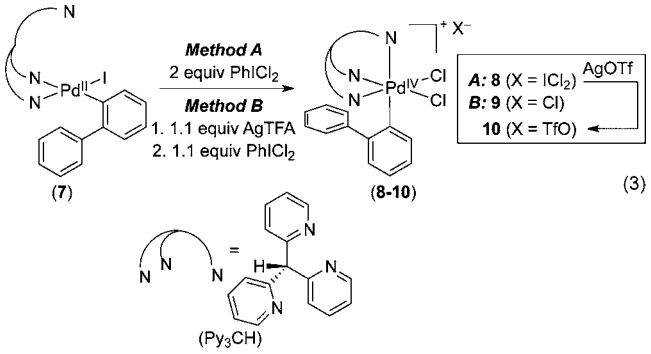

(3)

(I) (**7**) with 2 equiv of $PhICl_2$ in CH_2Cl_2 at room temperature (eq 3, method A) afforded the desired cationic Pd^{IV} product **8** in 85% yield as the ICl_2^- salt. The corresponding chloride salt (**9**) was obtained in 83% yield under slightly modified conditions (eq 3, method B). Finally, the treatment of **8** with 2 equiv of AgOTf resulted in smooth conversion to the triflate salt **10** in 90% yield. As predicted, complexes **8**−**10** were significantly more stable than **3**, and they could be stored in the solid state at room temperature for at least 4 weeks without detectable decomposition.

High resolution ESI mass spectrometric analysis of **8**−**10** showed an intense peak with m/z = 576.022, corresponding to the cationic Pd^{IV} core. The solution stereochemistry and conformations of **8**−**10** were elucidated via 1D ^1H NMR and 2D $^1H/^1H$ NOESY and ROESY NMR spectra. The ROESY NMR spectrum and peak assignments for **8** are shown in Figure 2. The most notable feature of this structure is the orientation of the phenyl ring of the biaryl ligand underneath two of the pyridine rings. This solution conformation was assigned on the basis of the

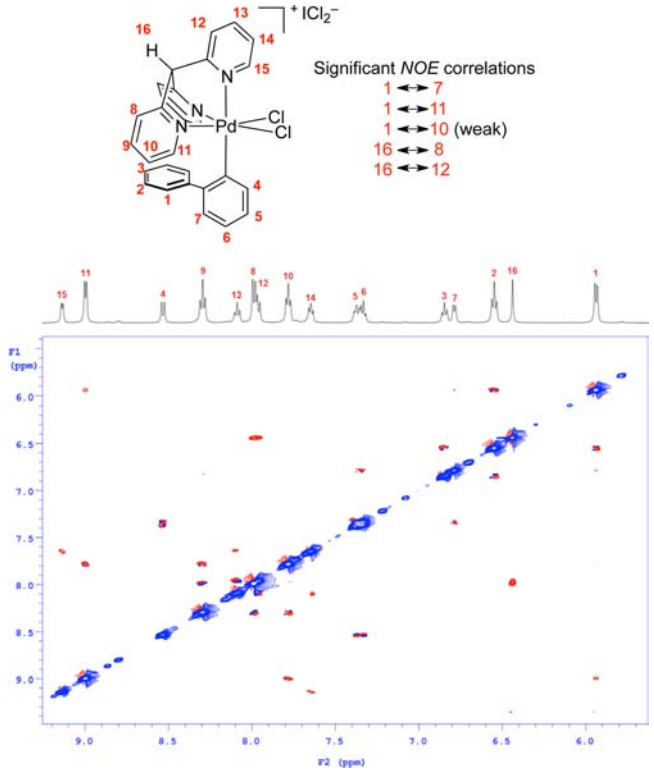

Figure 2. $^1H/^1H$ ROESY spectrum of **8** (CD_3NO_2; 25 °C; t_{mix} = 300 ms).

shielding of the aromatic protons H-1 and H-2 (to 5.9 and 6.6 ppm, respectively) as well as by NOE correlations between H-1 and H-10/H-11. An analogous conformation is observed in the solid state (vide infra). This conformational preference is likely due to favorable $\pi-\pi$ interactions between the biphenyl and tripyridylmethane ligands.

The ^1H NMR spectra of **8**−**10** show a large dependence on the counterion X. The spin−lattice relaxation times for **8** and **9** in $CDCl_3$ at 25 °C show that both ICl_2^- and Cl^- have close interactions with H-8, H-12, and H-16 of the Py_3CH ligand.[15] This is likely due to equilibration of the counterions between these three similar sites (eq 4). Remarkably, these interactions

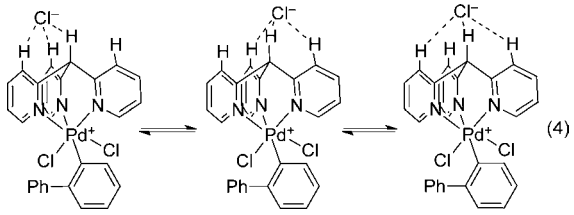

(4)

persist even in the polar solvent CD_3NO_2. In contrast, the triflate in complex **10** does not have strong interactions with the Py_3CH ligand in either $CDCl_3$ or CD_3NO_2.[15] Related binding of iodide, bromide and chloride to the ligand periphery of cationic Pd^{IV} complexes has been documented previously.[16]

The structure of complex **8** was further confirmed by single crystal X-ray diffraction analysis, and an ORTEP drawing of **8** is shown in Figure 3. In the solid state, the ICl_2^- counterion has short contacts with the methine hydrogen [Cl(3)−H(1) = 2.872 Å] as well as with pyridine proton H-2 [Cl(3)−H(2) = 2.752 Å; I−H(2) = 3.354 Å]. Furthermore, the phenyl ring of the biaryl is positioned closely underneath the Py_3CH ligand, consistent with the π-stacking interaction proposed on the basis of the solution NMR studies.[17,18]

dx.doi.org/10.1021/ja401557m | J. Am. Chem. Soc. 2013, 135, 6618−6625

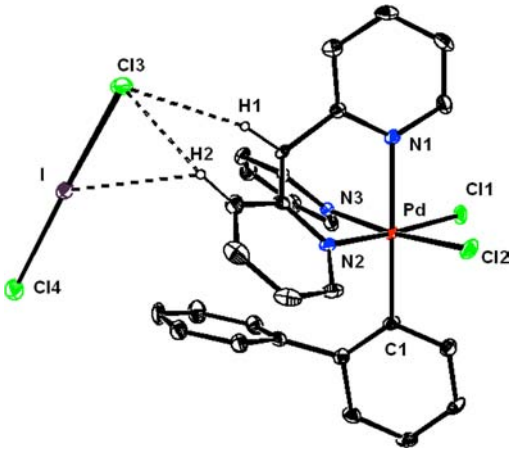

Figure 3. ORTEP drawing of complex **8**. Thermal ellipsoids are drawn at 50% probability. Only hydrogen atoms involved in short contact with ICl_2^- are shown for clarity. Selected bond lengths (Å): Pd−C(1) 2.087(3), Pd−Cl(1) 2.2904(7), Pd−N(1) 2.184(3), Pd−N(2) 2.043(3), Cl(3)−H(1) 2.872(3), Cl(3)−H(2) 2.751(8), I−H(2) 3.353(8). Selected bond angles (deg): N(2)−Pd−Cl(1) 88.32(7), Cl(1)−Pd−Cl(2) 90.12(3), Cl(2)−Pd−N(3) 89.82(7), N(3)−Pd−N(2) 91.27(8), N(1)−Pd−C(1) 178.87(11).

Reactivity of 8−10. On the basis of our previous work (eq 2),[10] we expected that heating complexes **8**−**10** would result in C−H activation to form products like **13** (eq 5a).

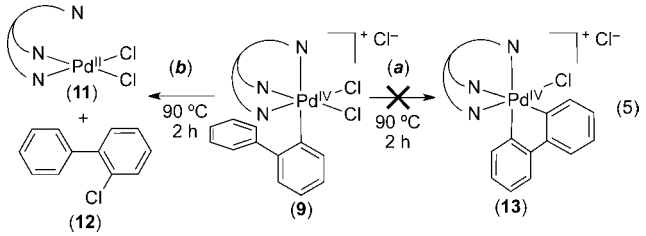

However, instead, heating **9** at 90 °C for 2 h in $CDCl_3$ resulted in C−Cl bond-forming reductive elimination to afford Pd^{II} complex **11** along with chlorobiphenyl **12** (eq 5b).

We next hypothesized that base might be necessary to promote C−H activation in this system. However, the treatment of **9** with an excess of triethylamine or pyridine in CH_2Cl_2 at room temperature for 4 h returned only unreacted starting material (eq 6b).[19]

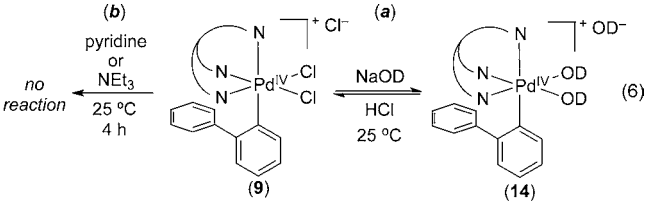

Complex **9** did react quantitatively with NaOD at 25 °C to form a colorless D_2O-soluble Pd^{IV} product that we propose to be the deuteroxide complex **14** (eq 6a). Attempts to isolate **14** resulted in decomposition; however, this complex was characterized in situ via $^{13}C\{^1H\}$, $^1H/^1H$ gCOSY, and NOESY NMR experiments as well as $^1H/^{13}C$ HSQC and HMBC correlation experiments. We formulate **14** as a monomer rather than an oxo or deuteroxo-bridged dimer on the basis of internal reference diffusion-ordered NMR (DOSY)[20] spectroscopic analysis.[21] Notably, the chloride-to-deuteroxide ligand exchange was completely reversible. The acidification of D_2O solutions of **14** with aqueous HCl resulted in rapid and near quantitative regeneration of **9**.

The observation of reversible chloride for deuteroxide ligand exchange prompted us to test the related ligand substitution reaction of chloride for acetate. We reasoned that incorporation of an acetate ligand might trigger acetate-assisted C−H activation at Pd^{IV}. Gratifyingly, the treatment of a $CDCl_3$ solution of **9** with 5% aqueous KOAc resulted in a rapid color change from orange to yellow within 5 min, and ^1H NMR analysis of the separated $CDCl_3$ layer showed clean conversion to the cyclometalated product **13**. When this reaction was performed on a preparative scale, **13** was isolated in only 39% yield. However, optimization of the conditions (through the use of anhydrous $CHCl_3$ as the solvent and substituting aqueous KOAc with AgOAc) led to the formation of **13** in 78% isolated yield after 5 min at 25 °C (eq 7).[22]

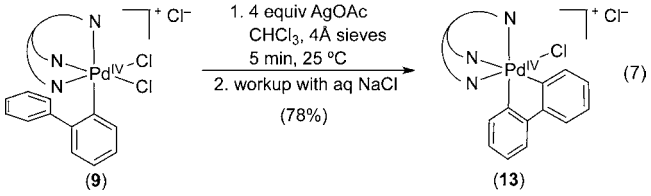

Complex **13** is stable at room temperature in the solid state and in $CDCl_3$ solution for at least two weeks. This cyclometalated compound was characterized using standard 1D and 2D NMR analysis as well as by single crystal X-ray diffraction. The X-ray structure of **13** is shown in Figure 4. In the solid-state, the chloride counterion is in short contact with the methine hydrogen (Cl(2)−H(1) = 2.568 Å) as well as with a cocrystallized water molecule.

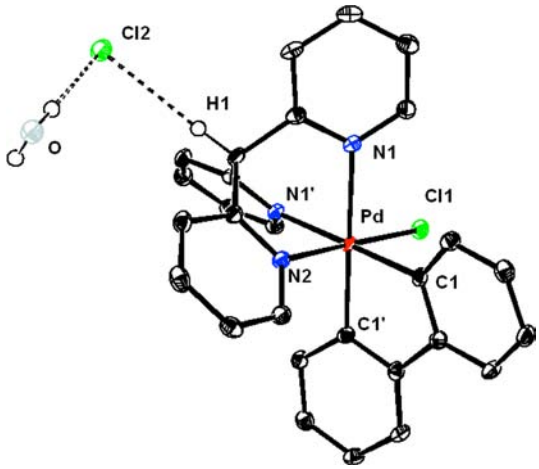

Figure 4. ORTEP drawing of complex **13**. Thermal ellipsoids are drawn at 50% probability. Only hydrogen atom involved in short contact with chloride counterion is shown for clarity. Selected bond lengths (Å): Pd−C(1) 2.1765(14), Pd−Cl(1) 2.2961(6), Pd−N(1) 2.1765(14), Pd−N(2) 2.049(2), H(1)−Cl(2) 2.238(17). Selected bond angles (deg): N(1)−Pd−Cl(1) 91.95(4), Cl(1)−Pd−C(1) 88.51(5), C(1)−Pd−N(2) 90.58(6), N(2)−Pd−N(1) 88.96(5), C(1)−Pd−C(1′) 81.47(9), N(1)−Pd−C(1) 179.14(6).

Proposed Mechanism of C−H Activation. We next sought to gain insights into the mechanism of this C−H activation reaction. As noted in eq 6 and 7, acetate was the only base examined that promoted this transformation. This strongly suggests that the carboxylate is not simply serving as an external base in the reaction. Furthermore, the observation of

dx.doi.org/10.1021/ja401557m | J. Am. Chem. Soc. 2013, 135, 6618−6625

facile replacement of chloride with hydroxide (eq 6) indicates the feasibility of ligand substitution to form a Pd^{IV} acetate intermediate prior to C−H activation. On the basis of these preliminary observations, we hypothesized that the observed C−H activation reaction could proceed via the pathway depicted in eq 8. This involves four distinct steps: (1) chloride-to-acetate

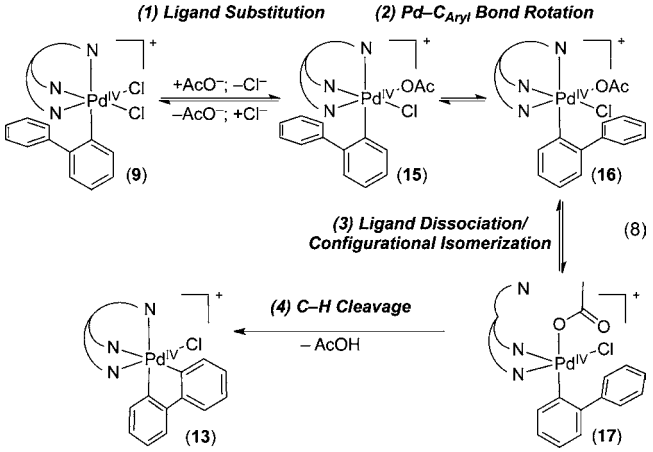

ligand substitution, (2) rotation about the Pd−C_{Aryl} bond, (3) pyridine ligand dissociation and configurational isomerization via Berry pseudorotation, and (4) acetate-assisted C−H cleavage. (Note that steps 2 and 3 could also occur in opposite order.) We have conducted a variety of experiments to assess the feasibility of each of the proposed steps. These studies are described in detail in the sections below.

Ligand Substitution. The first step of the proposed mechanism involves chloride to acetate ligand substitution at cationic Pd^{IV} complex **9**. This would be expected to proceed via reversible dissociation of one pyridine arm of the Py_3CH ligand followed by binding of acetate to generate intermediate **18** (eq 9).

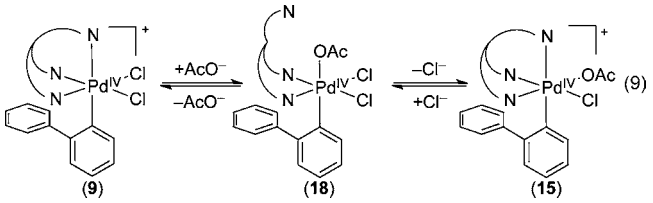

Subsequent chloride dissociation and reassociation of the pyridine arm would then yield **15**.

We first sought to detect **15** at low temperature using ^{1}H NMR spectroscopy. Treatment of a CD_2Cl_2 solution of **9** with 3 equiv of Bu_4NOAc at −20 °C resulted in the formation of a new species with spectroscopic features consistent with **15** (eq 10). This

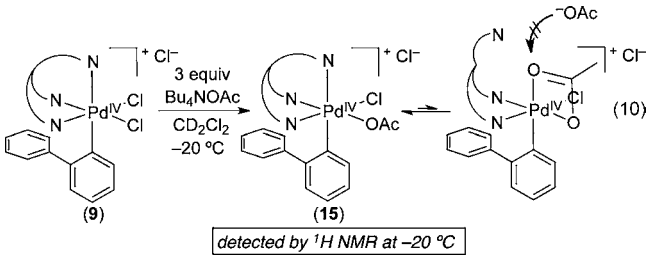

compound was unstable to isolation and underwent rapid C−H activation to form **13** upon warming to 0 °C. As such, **15** could only be characterized in situ by 1D ^{1}H NMR spectroscopy as well as 2D ^{1}H/^{1}H gCOSY and NOESY.[23] Several diagnostic spectral features support the assignment of this species as a monoacetate complex. Most importantly, the ^{1}H NMR spectrum shows that this intermediate lacks a plane of symmetry, suggesting that only one chloride ligand has undergone ligand exchange with an acetate. The observed substitution of only one of the chloride ligands is likely due to the possibility of κ^2 binding of the acetate to the cationic Pd^{IV} center (eq 10).[24] This binding mode would inhibit coordination of a second acetate.

In order to gain further insights into ligand exchange processes at **9**, we examined substitution reactions with other nucleophilic anions. As shown in eq 11, complex **9** underwent facile

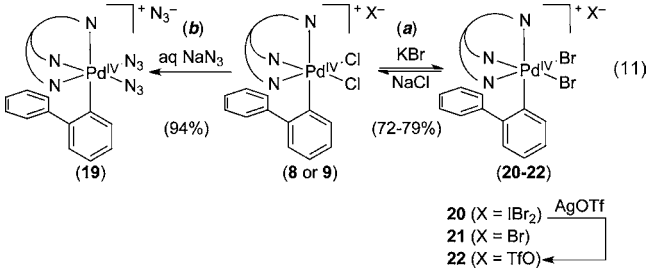

ligand exchange with both bromide and azide to generate stable products **19**−**22**.

Complexes **19**−**22** were characterized using conventional 1D and 2D NMR techniques as well as HRMS. All of these compounds show C_S symmetry, which indicates that both chloride ligands have been exchanged. Notably, the ^{1}H NMR spectrum of **19** shows several equilibrating species, suggesting that it exists as a mixture of conformational and configurational isomers (vide infra for further discussion). In contrast, the ^{1}H NMR spectra of **20**−**22** are each consistent with the presence of a single major isomer in solution. These latter spectra are extremely similar to that of **8**. The identity of complex **20** was further confirmed by single crystal X-ray diffraction analysis, and the structure is shown in Figure 5. Interestingly, in this case

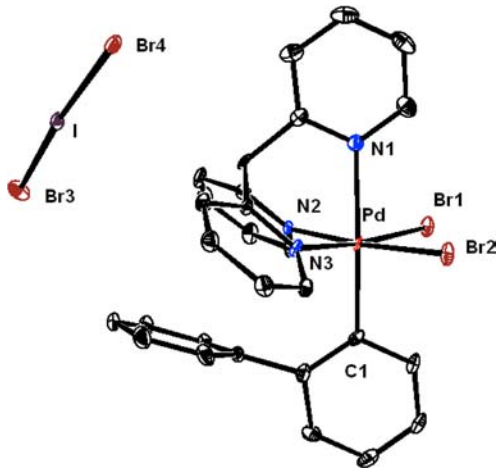

Figure 5. ORTEP drawing of complex **20**. Thermal ellipsoids are drawn at 50% probability. Hydrogen atoms are omitted for clarity. Selected bond lengths (Å): Pd−C(1) 2.092(3), Pd−Br(1) 2.4267(5), Pd−N(1) 2.199(3), Pd−N(2) 2.070(3). Selected bond angles (deg): N(2)−Pd−Br(1) 88.74(8), Br(1)−Pd−Br(2) 89.707(15), Br(2)−Pd−N(3) 89.17(8), N(3)−Pd−N(2) 91.88(10), N(1)−Pd−C(1) 177.49(13).

the IBr_2^- counterion is not in short contact with the cationic Pd^{IV} core.

dx.doi.org/10.1021/ja401557m | J. Am. Chem. Soc. 2013, 135, 6618−6625

The chloride to bromide ligand exchange was readily reversible, and **20**–**22** reacted rapidly (within 5 min at 25 °C) with aqueous NaCl to regenerate **9** (eq 11a). The presence of bromide ligands did not alter the reactivity of the Pd^{IV} center toward carboxylate-assisted C–H activation. For example, the reaction of **22** with 4 equiv of AgOAc resulted in clean C–H cleavage to afford cyclometalated product **23** in 53% isolated yield (eq 12a). In

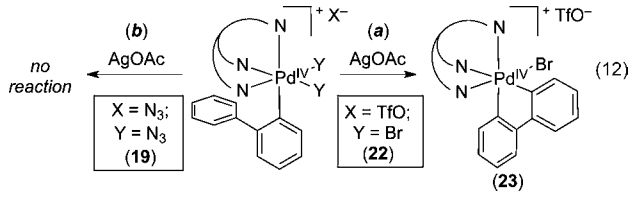

contrast, the equilibrium for chloride to azide exchange appears to lie far to the left, as no reaction was observed upon treatment of **19** with a large excess of aqueous NaCl (eq 11b). In addition, the treatment of azide complex **19** with AgOAc returned only unreacted starting material (eq 12b).

The proposed ligand substitution (step 1 in eq 8) as well as the configurational isomerization (step 3 in eq 8) both involve reversible dissociation of one arm of the Py_3CH ligand. We thus hypothesized that these two steps (and therefore potentially the overall C–H activation process) would be slowed significantly by replacing the Py_3CH ligand with Py_3CCH_3 (complex **24** in eq 13). The additional methyl group in Py_3CCH_3 is expected

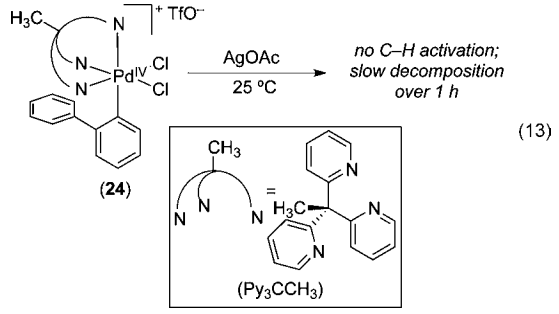

to render **24** more rigid than Py_3CH, thereby hindering the pyridine dissociation process.

Complex **24** was synthesized using a similar procedure to that for **10**. As predicted, this complex showed dramatically reduced reactivity toward acetate-assisted C–H activation. The treatment of **24** with AgOAc or aqueous KOAc at room temperature did not lead to cyclometalation (eq 13). Instead, these conditions resulted in slow (over 1 h) decomposition of **24** to generate a complex mixture of products.

To directly compare ligand substitution at **24** and **10**, we studied the reaction of both complexes with KBr (eq 14). The reactions

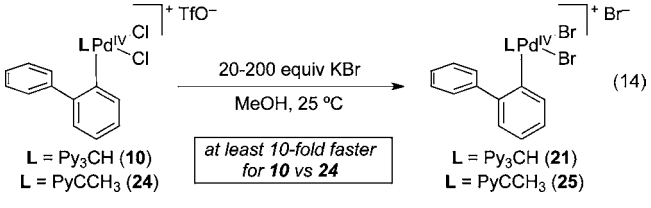

were monitored via UV–vis spectroscopy based on the appearance of an absorbance band at 480 nm. Because the overall transformation shown in eq 14 involves multiple elementary steps, the obtained reaction traces could not be fitted to simple rate laws.[25]

Despite this complexity, the experiments showed that, under otherwise identical reaction conditions, ligand substitution of Cl for Br at **10** proceeds to completion more than 10-fold faster than the analogous transformation at **24**. This is consistent with our predictions about the increased rigidity of Py_3CCH_3 compared to Py_3CH.

Rotation about the Pd^{IV}–C_{Aryl} Bond. As discussed above, complexes **8**–**10** were obtained as a single conformer with respect to rotation about the Pd–biphenyl bond. The favored conformation has the biphenyl ligand positioned under the Py_3CH group. We hypothesize that this conformation is stabilized by π-stacking between the electron-rich phenyl group of the biphenyl and the electron deficient pyridines. In an effort to disrupt this π–π interaction, we synthesized a complex containing three electron-withdrawing fluorine substituents on the biphenyl ligand (**26**). As anticipated, this compound exists as a mixture of two C_S symmetric conformational isomers **26a** and **26b** (**26a**:**26b** = 40:60 in $CDCl_3$, eq 15). The identity of each isomer was established using 1D ^1H

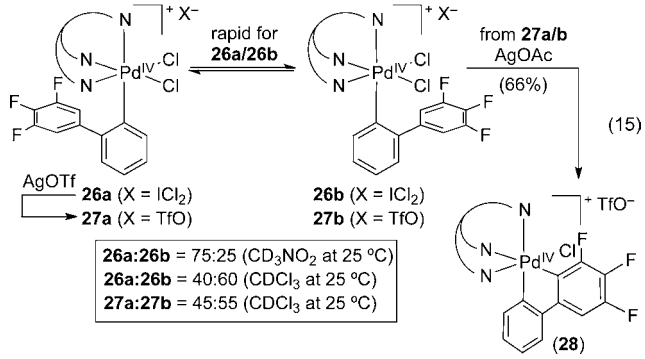

NMR and 2D $^1H/^1H$ ROESY NMR spectroscopy. In addition, an EXSY experiment revealed that **26a** and **26b** interconvert on the NMR time scale.[26] Collectively, these results show that rotation around the Pd–aryl bond is fast in **26** and that both conformations are readily accessible at room temperature.[27]

As shown in eq 15, both complex **26** and its triflate counterpart **27** participate in acetate-assisted C–H activation in a similar fashion to **8**–**10**. For example, the treatment of **27a,b** with 4 equiv of AgOAc in dry $CHCl_3$ afforded product **28** in 66% isolated yield.[28] Overall this series of experiments demonstrates the feasibility of rotation about the Pd^{IV}–aryl bond in complexes that undergo acetate-assisted C–H activation (and that are closely related to the parent compounds **8**–**10**).

Configurational Isomerization via Berry Pseudorotation. The viability of the proposed configurational isomerization process was first probed by EXSY NMR experiments in complexes of general structure $[(Py_3CH)Pd(biphenyl)Y_2]^+$.[26] Only one isomer is observed in the ^1H and ^{13}C NMR spectra of dichloride complexes **8**–**10**; furthermore, $^1H/^1H$ ROESY and NOESY experiments show that **8**–**10** are configurationally stable on the NMR time scale. In contrast, the $^1H/^1H$ ROESY spectrum of dibromide complex **20** (Figure 6) shows chemical exchange cross peaks between the two equivalent pyridine rings trans to the bromides and the one distinct pyridine ring trans to the carbon.

It is well documented that six-coordinate complexes can undergo inversion of configuration at the metal via bond-rupture and generation of a configurationally labile five-coordinate intermediate.[29] We propose that the observed exchange in complex **20** is the result of such a pathway. As depicted in eq 16, initial dissociation of one arm of the facial tridentate pyridine ligand (labeled N^2 in eq 16)

dx.doi.org/10.1021/ja401557m | J. Am. Chem. Soc. 2013, 135, 6618–6625

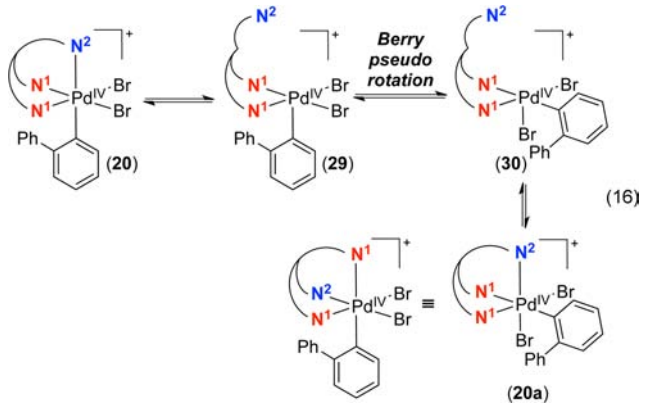

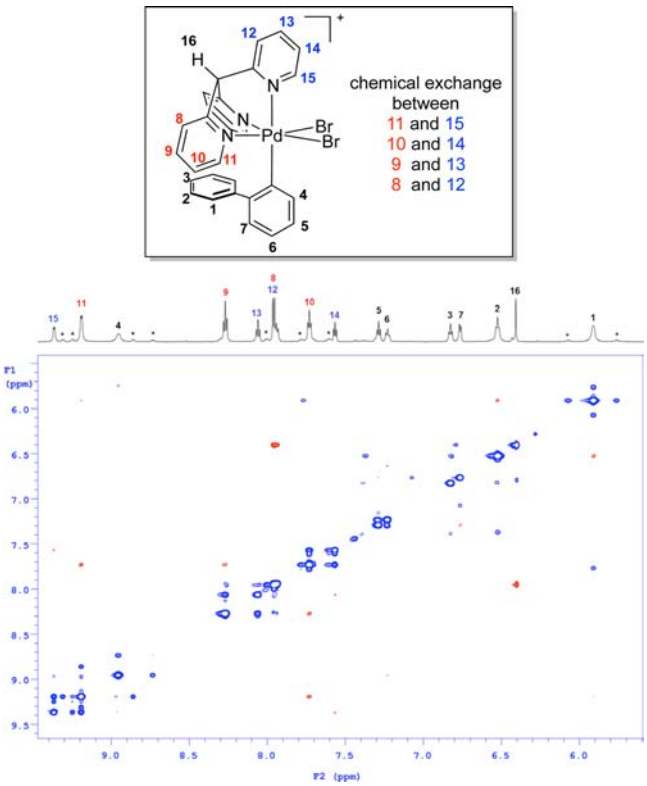

Figure 6. 2D ^{1}H/^{1}H ROESY NMR spectrum of **20**. 1D trace and peak assignments are provided above. The peaks marked with * are low intensity resonances associated with an unknown species that is in fast exchange with **20**.

would afford the 5-coordinate complex **29**, which could undergo configurational isomerization to form **30** via Berry pseudorotation.[30] Reassociation of N^2 would then afford product **20a**. Importantly, complexes **20** and **20a** are chemically equivalent, with the sole difference that N^2 has swapped places with one of the N^1 groups. The configurational isomerization pathway proposed in eq 16 is further supported by the observation of broad, low intensity resonances in the ^{1}H NMR and ^{1}H/^{1}H ROESY spectra of **20** (labeled with asterisks in Figure 6). This species is in fast exchange with **20** on the NMR time scale. Although the broad signals make it difficult to characterize definitively, we propose that this could be an intermediate like **29** or **30**.[31−33]

As discussed above, the Py_3CCH_3 ligand was predicted to render the Pd center less reactive toward ligand dissociation, the first step of the configurational isomerization process in eq 16. Indeed, the ROESY NMR spectrum of $[(Py_3CCH_3)Pd(Br)_2(biphenyl)]Br$ (**25**) shows no analogous chemical exchange cross-peaks, indicating that this exchange process is significantly slower than in the corresponding Py_3CH adduct **20**. This provides additional support for the exchange pathway involving reversible dissociation of an arm of the pyridine ligand.

Acetate Assisted C−H Cleavage. A series of isotope effect studies were conducted to gain insights into the nature of the transition state for C−H cleavage as well as to establish whether C−H bond activation is involved in the rate-determining step of the overall transformation.[34] Monodeuterated complex **31** was synthesized by analogy to the procedure shown in eq 3.[35] Complex **31** was then treated with various carboxylate sources to yield the cyclopalladated product **32** (eq 17). ^{1}H NMR analysis of

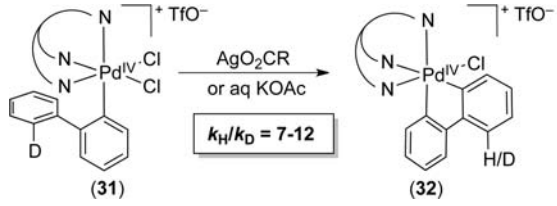

32 showed that cleavage of the C−H bond occurs in preference to cleavage of the C−D bond with all of the carboxylates examined. Accurate values for the intramolecular isotope effect were obtained via ESI mass spectrometric analysis. All of the carboxylate sources tested [KOAc (aqueous), AgOAc, AgOPiv, AgO_2CCF_3, and $AgO_2CC_6H_5$] afforded product **32** with an intramolecular k_H/k_D between 9 and 12 at 25 °C. Increasing the reaction temperature to 55 °C and lowering it to 0 °C had a relatively small influence on the observed isotope effect. For example, with AgOAc, k_H/k_D = 10 at 0 °C and 7 at 55 °C. These latter results indicate that quantum tunneling does not contribute significantly to the isotope effect in this system.[36] Overall, the observed large magnitude of the intramolecular isotope effect is indicative of a central transition state for C−H cleavage, suggesting that the proton is transferred between two sites of similar basicity.[37] The observed values are similar to those reported for carboxylate-assisted C−H cleavage at Pd(II)[4d] and Ir(III)[7b] centers (values in the literature vary from 5 to 7).

The intermolecular KIE for this reaction was next determined using substrates **33** and **36** (eq 18). The *t*-butyl group was

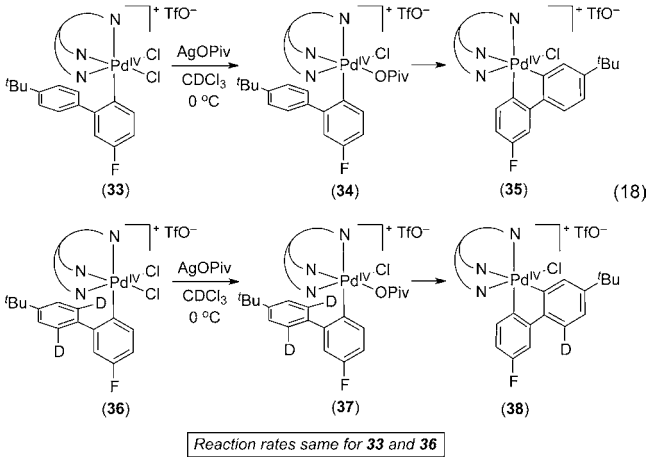

introduced on the biphenyl ligand of **33** and **36** in order to enhance solubility (essential for obtaining quantitative rate data). The fluorine substituent was added to enable monitoring of the

dx.doi.org/10.1021/ja401557m | J. Am. Chem. Soc. 2013, 135, 6618−6625

reaction rate using ^{19}F NMR spectroscopy.[38] The treatment of **33** and **36** with 3 equiv of AgOPiv resulted in smooth conversion to cyclopalladated products **35** and **38**. The progress of these reactions was monitored by ^{19}F NMR spectroscopy. After 5 min, both substrates **33** and **36** underwent nearly quantitative conversion to the monopivalate intermediates **34** and **37**. Both intermediates **34** and **37** then underwent relatively slow conversion to **35** and **38**, respectively. The overall reaction rates for substrates **33** and **36** under these conditions were the same within the error of measurement. These observations show that the rate of the overall transformation is not limited by the rate of the ligand exchange or the availability of the carboxylate ligand and that either conformational or configurational isomerization is likely the rate-limiting step in this transformation.

■ CONCLUSIONS

This paper describes a detailed investigation of carboxylate-assisted C−H activation at Pd^{IV} centers. As discussed above, we propose a pathway involving four steps: (1) ligand exchange, (2) Pd−C_{Aryl} bond rotation, (3) configurational isomerization via Berry pseudorotation, and (4) carboxylate-assisted C−H cleavage. The feasibility of each of these steps is supported by the experiments presented above. A key feature of the investigated [(Py_3CH)Pd(biphenyl)Cl_2]X system is the semilabile tridentate tris(2-pyridyl)methane ligand. This ligand stabilizes octahedral cationic Pd^{IV} centers toward reductive elimination. However, coordinatively unsaturated species can be accessed readily via dissociation of a pyridine arm of the ligand. This ligand dissociation is believed to facilitate the key ligand exchange and configurational isomerization steps. Importantly, the extremely mild conditions necessary for acetate assisted C−H cleavage at Pd^{IV} centers renders this process attractive for applications in catalytic C−H functionalization processes mediated by high oxidation state palladium. Ongoing investigations are focused on expanding this reactivity to other octahedral high valent group 10 metal centers and to conducting detailed investigations of the factors governing site selectivity in these transformations.

■ ASSOCIATED CONTENT

Supporting Information

Experimental details and crystallographic (CIF) and spectroscopic data for new compounds. This material is available free of charge via the Internet at http://pubs.acs.org.

■ AUTHOR INFORMATION

Corresponding Author

mssanfor@umich.edu

Notes

The authors declare no competing financial interest.

■ ACKNOWLEDGMENTS

We thank the NSF (CHE-1111563) for support of this research. We also acknowledge funding from NSF Grant CHE-0840456 for X-ray instrumentation. A.M. is a Howard Hughes Medical Institute International Student Research Fellow.

■ REFERENCES

(1) For recent reviews, see: (a) Lyons, T. W.; Sanford, M. S. *Chem. Rev.* **2010**, *110*, 1147−1169. (b) Ackermann, L. *Chem. Rev.* **2011**, *111*, 1315−1345. (c) Yamaguchi, J.; Yamaguchi, A. D.; Itami, K. *Angew. Chem., Int. Ed.* **2012**, *51*, 8960−9009. (d) Neufeldt, S. R.; Sanford, M. S. *Acc. Chem. Res.* **2012**, *45*, 936−946.

(2) Ryabov, A. D.; Sakodinskaya, I. K.; Yatsimirsky, A. K. *J. Chem. Soc., Dalton Trans.* **1985**, 2629−2638.

(3) Lafrance, M.; Gorelsky, S. I.; Fagnou, K. *J. Am. Chem. Soc.* **2007**, *129*, 14570−14571.

(4) (a) Lapointe, D.; Fagnou, K. *Chem. Lett.* **2010**, *39*, 1118−1126. (b) Gorelsky, S.; Lapointe, D.; Fagnou, K. *J. Org. Chem.* **2012**, *77*, 658−668. (c) Gorelsky, S. I.; Stuart, D. R.; Campeau, L.-C.; Fagnou, K. *J. Org. Chem.* **2010**, *75*, 8180−8189. (d) D. García-Cuadrado, D.; Braga, A. A. C.; Maseras, F.; Echavarren, A. M. *J. Am. Chem. Soc.* **2006**, *128*, 1066−1067.

(5) Davies, D. L.; Donald, S. M. A.; Macgregor, S. A. *J. Am. Chem. Soc.* **2005**, *127*, 13754−13755.

(6) For carboxylate-assisted C−H activation at Rh^{III}, see: Rhinehart, J. L.; Manbeck, K. A.; Buzak, S. K.; Lippa, G. M.; Brennessel, W. W.; Goldberg, K. I.; Jones, W. D. *Organometallics* **2012**, *31*, 1943−1952.

(7) For carboxylate-assisted C−H activation at Ir^{III}, see: (a) Davies, D. L.; Donald, S. M. A.; Al-Duaij, O.; Macgregor, S. A.; Pölleth, M. *J. Am. Chem. Soc.* **2006**, *128*, 4210−4211. (b) Li, L.; Brennessel, W. W.; Jones, W. D. *Organometallics* **2009**, *28*, 3492−3500.

(8) For carboxylate-assisted C−H activation at Ru^{II}, see: Davies, D. L.; Al-Duaij, O.; Fawcett, J.; Giardiello, M.; Hilton, S. T.; Russell, D. R. *Dalton Trans.* **2003**, 4132−4138.

(9) (a) Juwaini, N. A. B.; Ng, J. K. P.; Seayad, J. *ACS Catal.* **2012**, *2*, 1787−1791. (b) Wang, X.; Leow, D.; Yu, J.-Q. *J. Am. Chem. Soc.* **2011**, *133*, 13864−13867. (c) Hickman, A. J.; Sanford, M. S. *ACS Catal.* **2011**, *1*, 170−174. (d) Sibbald, P. A.; Rosewall, C. F.; Swartz, R. D.; Michael, F. E. *J. Am. Chem. Soc.* **2009**, *131*, 15945−15951. (e) Rosewall, C. F.; Sibbald, P. A.; Liskin, D. V.; Michael, F. E. *J. Am. Chem. Soc.* **2009**, *131*, 9488−9489. (f) Pilarski, L. T.; Selander, N.; Bose, D.; Szabo, K. J. *Org. Lett.* **2009**, *11*, 5518−5521. (g) Hull, K. L.; Lanni, E. L.; Sanford, M. S. *J. Am. Chem. Soc.* **2006**, *128*, 14047−14049.

(10) Racowski, J. M.; Ball, N. D.; Sanford, M. S. *J. Am. Chem. Soc.* **2011**, *133*, 18022−18025.

(11) Examples of Pd^{IV} complexes supported by neutral tridentate (L_3-type) ligands: (a) Klaui, W.; Glaum, M.; Wagner, T.; Bennett, M. A. *J. Organomet. Chem.* **1994**, *472*, 355−358. (b) Bennett, M. A.; Canty, A. J.; Felixberger, J. K.; Rendina, L. M.; Sutherland, C.; Willis, A. C. *Inorg. Chem.* **1993**, *32*, 1951−1958. (c) Brown, D. G.; Byers, P. K.; Canty, A. J. *Organometallics* **1990**, *9*, 1231−1235.

(12) Examples of Pd^{IV} tris(pyrazoyl)borate complexes: (a) Campora, J.; Palma, P.; del Rio, D.; Lopez, J. A.; Alvarez, E. *Organometallics* **2005**, *24*, 3624−3628. (b) Canty, A. J.; Jin, H.; Penny, J. D. *J. Organomet. Chem.* **1999**, *573*, 30−35. (c) Canty, A. J.; Jin, H.; Roberts, A. S.; Skelton, B. W.; White, A. H. *Organometallics* **1996**, *15*, 5713−5722.

(13) Examples of Pd^{IV} pincer complexes: (a) Vicente, J.; Arcas, A.; Julia-Hernandez, F.; Bautista, D. *Inorg. Chem.* **2011**, *50*, 5339−5341. (b) Vicente, J.; Arcas, A.; Julia-Hernandez, F.; Bautista, D. *Angew. Chem., Int. Ed.* **2011**, *50*, 6896−6899. (c) Vicente, J.; Arcas, A.; Julia-Hernandez, F.; Bautista, D. *Chem. Commun.* **2010**, *46*, 7253−7255. (d) Canty, A. J.; Rodemann, T.; Skelton, B. W.; White, A. H. *Organometallics* **2006**, *25*, 3996−4001. (e) Lagunas, M.-C.; Gossage, R. A.; Spek, A. L.; van Koten, G. *Organometallics* **1998**, *17*, 731−741. (f) Alsters, P. L.; Engel, P. F.; Hogerheide, M. P.; Copijn, M.; Spek, A. L.; van Koten, G. *Organometallics* **1993**, *12*, 1831−1844.

(14) (a) Byers, P. K.; Canty, A. J.; Skelton, B. W.; White, A. H. *Organometallics* **1990**, *9*, 826−832. (b) Byers, P. K.; Canty, A. J.; Skelton, B. W.; White, A. H. *J. Chem. Soc., Chem. Commun.* **1987**, 1093−1095.

(15) See pages S231−S235 in Supporting Information Document 4 for full details.

(16) (a) McCall, A. S.; Wang, H.; Desper, J. M.; Kraft, S. *J. Am. Chem. Soc.* **2011**, *133*, 1832−1848. (b) Brown, D. G.; Byers, P. K.; Canty, A. J. *Organometallics* **1990**, *9*, 1231−1235.

(17) The phenyl ring and pyridine rings of the Py_3CH ligand in complex **8** are offset, which is known to be the most favorable π-stacking geometry. For detailed discussion on π-stacking interactions and geometries, see: Hunter, C. A.; Sanders, J. M. K. *J. Am. Chem. Soc.* **1990**, *112*, 5525−5534.

(18) The interplane angles between the phenyl ring of the biphenyl ligand and pyridine rings of the Py_3CH ligand in complex **8** are 28.3 and 39.7 degrees. The distances between the centroid of the phenyl ring of the biphenyl ligand and centroids of the pyridine rings of the Py_3CH ligand are 3.754 Å and 4.206 Å. Such centroid−centroid separations (R_{cen}) are typical for aromatic rings involved in parallel π-stacking interactions. For statistical analysis of X-ray data on R_{cen} for aromatic rings involved in π-stacking see: McGaughey, G. B.; Gagné, M.; Rappé, A. K. *J. Biol. Chem.* **1998**, *273*, 15458−15463.

(19) When this reaction was conducted at 60 °C, complex **10** underwent decomposition to generate a complex mixture of unidentified products. The desired product **14** was not detected.

(20) (a) Li, D.; Kagan, G.; Hopson, R.; Williard, P. G. *J. Am. Chem. Soc.* **2009**, *131*, 5627−5634. (b) Li, W.; Kagan, G.; Yang, H.; Cai, C.; Hopson, R.; Sweigart, D. A.; Williard, P. G. *Org. Lett.* **2010**, *12*, 2698−2701.

(21) See pages S170−S172 in Supporting Information Document 4 for full details.

(22) When complex **9** was treated with 10 equiv of $AgBF_4$ in $CDCl_3$ solution (sonication for 1 h and stirring at room temperature for 24 h), only abstraction of the outer sphere chloride counterion occurred, and no cyclopalladated product **13** was formed as determined by ^1H NMR. When $AgSbF_6$ was used instead of $AgBF_4$, the starting material **9** decomposed to a complex mixture of products, none of which was the anticipated cyclopalladated product **13**. These results show that acetate rather than silver ions promotes the C−H cleavage reaction.

(23) We used 6 sterically and electronically distinct carboxylates to promote C−H cleavage (vide infra). In addition to monocarboxylates we have also tested several dicarboxylates such as oxalate, malonate, succinate, and glutarate. None of these mono- or dicarboxylates afforded an intermediate that was stable enough to be isolated and completely characterized.

(24) For examples of Pd^{II} κ^2-acetate complexes, see: (a) Thirupathi, N.; Amoroso, D.; Bell, A.; Protasiewicz, J. D. *Organometallics* **2005**, *24*, 4099−4102. (b) Viciu, M. S.; Stevens, E. D.; Petersen, J. L.; Nolan, S. P. *Organometallics* **2004**, *23*, 3752−3755. (c) Lee, J.-C.; Wang, M.-G.; Hong, F.-E. *Eur. J. Inorg. Chem.* **2005**, 5011−5017.

(25) See pages S235−S236 in Supporting Information Document 4 for full details.

(26) Perrin, C. L.; Dwyer, T. J. *Chem. Rev.* **1990**, *90*, 935−967.

(27) Surprisingly, the isomeric triflate complexes **27a** and **27b** do not interconvert on the NMR time scale. This observation indicates that the counterion can influence flexibility of the cationic Pd^{IV} core.

(28) Complex **26** also undergoes acetate-assistated C−H activation under analogous conditions. However, in this case, the isolated product was contaminated with approximately 15% of an unidentified side product that could not be removed by crystallization.

(29) (a) Heard, P. *J. Chem. Soc. Rev.* **2007**, *36*, 551−569. (b) Braustein, P.; Naud, F. *Angew. Chem., Int. Ed.* **2001**, *40*, 680−699. (c) Álvarez, C. M.; Carrillo, R.; García-Rodríguez, R.; Miguel, D. *Chem. Commun.* **2011**, *47*, 12765−12767. (d) Abel, W. E.; Kite, K.; Perkins, P. S. *Polyhedron* **1987**, *6*, 549−562. (e) Yang, H.; Alvarez-Gressier, M.; Lugan, N.; Mathieu, R. *Organometallics* **1997**, *16*, 1401−1409.

(30) (a) Berry, R. S. *J. Chem. Phys.* **1960**, *32*, 933−938. (b) Fortman, J. J. *Coord. Chem. Rev.* **1971**, *6*, 331−375.

(31) We disfavor formulation of this species as an octahedral tribromide complex on the basis of the fact that the addition of 2−4 equiv of NBu_4Br did not increase the equilibrium population of this compound in solution.

(32) The exchange processes described above can be observed for both complexes **19** and **20** using ROESY spectroscopy. In contrast, analogous exchange does not occur on the NMR time scale for chloride complex **8**. This is likely due to the strong π-donor ability of azide and bromide ligands as well as their larger size compared to chloride. Strong π-donors such as bromide should decrease ligand-field strength and ligand-field activation energy [which is relatively high for d^6 Pd^{IV}] and thereby facilitate dissociation of one pyridine arm of the hemilabile Py_3CH ligand. This proposal is supported by the observation that the Pd-N1 bond in dibromide complex **20** is 0.014 Å longer than in dichloride complex **8**. Furthermore, the Pd-N2 bond in **20** is 0.027 Å longer than in **8**. This data indicates that the more π-donating bromide has a stronger cis and trans influence than the chloride. It is very likely that the trans influence correlates with the trans effect in Pd^{IV} d^6 complexes such as **8** and **20**.

(33) Interestingly, no chemical exchange crosspeaks were detected in the $^1H/^1H$ ROESY spectrum for $[(Py_3CH)Pd(biphenyl)Br_2][TfO]$ (**22**). This observation demonstrates the influence of the outer-sphere counterion on the inner sphere Py_3CH ligand. A possible explanation for this observation is that hydrogen bonding of IBr_2^- with the Py_3CH ligand in complex **20** promotes dissociation of one pyridine ring and stabilizes a pentacoordinate intermediate like **32** or **33**.

(34) Gómez-Gallego, M.; Sierra, M. A. *Chem. Rev.* **2011**, *111*, 4857−4963.

(35) Analysis of **31** by ESI-MS showed that this complex is >99% monodeuterated. For details of analysis, see: Gruber, C. C.; Oberdorfer, G.; Voss, C. V.; Kremsner, J. M.; Kappe, C. O.; Kroutil, W. *J. Org. Chem.* **2007**, *72*, 5778−5783.

(36) (a) Anslyn, E. V.; Dougherty, D. A. *Modern Physical Organic Chemistry*; University Science Books: Sausalito, CA, 2006; pp 435−437. (b) McKinnon, W. R.; Hurd, C. M. *J. Phys. Chem.* **1983**, *87*, 1283−1285. (c) Limbach, H.-H.; Lopez, J. M.; Kohen, A. *Philos. Trans. R. Soc., B* **2006**, *361*, 1399−1415.

(37) (a) Sühnel, J. *J. Phys. Org. Chem.* **1990**, *3*, 62−68. (b) Bordwell, F. G.; Boyle, W. J., Jr. *J. Am. Chem. Soc.* **1975**, *97*, 3447−3452.

(38) The use of Bu_4NOAc or $AcOH/Et_3N$ resulted in formation of cyclopalladated products **35** or **38** in only 65 and 35% yield, respectively. Competitive formation of unidentified side products precluded the determination of reliable rate constants for C−H activation under these conditions.